TOXICOLOGICAL SCIENCES **134(2)**, 243–250 2013
doi:10.1093/toxsci/kft123
Advance Access publication June 7, 2013

# Generation and Characterization of a *Cyp4b1* Null Mouse and the Role of CYP4B1 in the Activation and Toxicity of Ipomeanol

Oliver T. Parkinson,* H. Denny Liggitt,† Allan E. Rettie,* and Edward J. Kelly‡,[1]

*Department of Medicinal Chemistry, †Department of Comparative Medicine, and ‡Department of Pharmaceutics, School of Pharmacy and Medicine, University of Washington, Seattle, Washington 98195-7610

[1]To whom correspondence should be addressed at Department of Pharmaceutics, School of Pharmacy and Medicine, University of Washington, Box 357610, 1959 North East Pacific Street, Seattle, WA 98195-7610. Fax: 206-543-3204. E-mail: edkelly@uw.edu.

Received February 20, 2013; accepted April 22, 2013

**4-Ipomeanol (IPO) is a prototypical pulmonary toxin that requires P450-mediated metabolic activation to reactive intermediates in order to elicit its toxic effects. CYP4B1 is a pulmonary enzyme that has been shown, *in vitro*, to have a high capacity for bioactivating IPO. In order to determine, unambiguously, the role of CYP4B1 in IPO bioactivation *in vivo*, we generated *Cyp4b1* null mice following targeted disruption of the gene downstream of exon 1. *Cyp4b1*$^{-/-}$ mice are viable and healthy, with no overt phenotype, and no evidence of compensatory upregulation of other P450 isoforms in any of the tissues examined. Pulmonary and renal microsomes prepared from male *Cyp4b1*$^{-/-}$ mice exhibited no detectable expression of the protein and catalyzed the *in vitro* bioactivation of IPO at < 10% of the rates observed in tissue microsomes from *Cyp4b1*$^{+/+}$ animals. Administration of IPO (20 mg/kg) to *Cyp4b1*$^{+/+}$ mice resulted in characteristic lesions in the lung, and to a lesser extent in the kidney, which were completely absent in *Cyp4b1*$^{-/-}$ mice. We conclude that CYP4B1 is a critical enzyme for the bioactivation of IPO *in vivo* and that the *Cyp4b1*$^{-/-}$ mouse is a useful model for studying CYP4B1-dependent metabolism and toxicity.**

***Key Words:*** **knockouts; cytochrome P450; metabolic activation; lung; pulmonary or respiratory system.**

4-Ipomeanol (IPO; 1-(3-furyl)-4-hydroxy-1-pentanone) is a furanoterpenoid toxin produced by sweet potatoes (*Ipomoea batatas*) in response to infection by the mold *Fusariam solani* (Doster *et al.*, 1978). IPO was discovered following poisoning of bovine livestock that developed severe interstitial pneumonia following ingestion of spoiled sweet potatoes (Doster *et al.*, 1978; Garst *et al.*, 1985). However, the pulmonary toxicity of IPO extends to a number of species beyond animal livestock, including many commonly used laboratory animals (Doster *et al.*, 1978; Garst *et al.*, 1985).

IPO is a protoxin that requires metabolic activation to elicit its toxic effects (Boyd, 1976). The first evidence that cytochrome P450 was involved in the bioactivation of IPO was provided by Boyd and Burka (1978) at the National Institutes of Health (NIH) in 1978, who showed that production of an alkylating metabolite by rat lung and liver microsomes depended upon NADPH and oxygen and was inhibited by carbon monoxide and chemical inhibitors of the P450 system. Subsequently, the same group demonstrated protection against covalent binding of IPO to target pulmonary cell types with a similar chemical inhibitor strategy (Devereux *et al.*, 1982). Following the successful purification of multiple pulmonary P450 isoforms from rabbits, Philpot and coworkers demonstrated that covalent binding of electrophilic species derived from IPO to protein and to glutathione occurred with two lung P450s that they termed P450I and P450II, known today as CYP2B4 and CYP4B1, respectively (Wolf *et al.*, 1982).

The first study to investigate IPO bioactivation by human P450s, performed with recombinant enzymes expressed in HepG2 cell lysates, identified several potential bioactivating P450 enzymes: CYP1A2, CYP2B7, CYP2F1, CYP3A3, and CYP3A4 (Czerwinski *et al.*, 1991). Interestingly, in that study, CYP1A2 was, by far, the most active human P450 enzyme for conversion of IPO to reactive metabolites that bound to calf thymus DNA. More recently, Baer *et al.* (2005) reported that human CYP1A2, CYP2C19, CYP2D6, CYP2E1, and CYP3A4 were the most active human P450s for metabolism of IPO to a reactive ene-dial that was trapped as a stable pyrrole adduct by N-acetylcysteine (NAC) and N-acetyllysine (NAL).

Clearly, bioactivation of IPO *in vitro* can be catalyzed by a wide variety of P450 enzymes. However, extrapolation of these data to the *in vivo* situation is complicated in several ways. First, it is often unclear exactly which P450 isoforms are present in target tissues at sufficiently high concentrations to cause protoxin activation with subsequent tissue damage to the intact organism. Second, all *in vitro* data for IPO bioactivation that are available to date have been conducted at a single high IPO concentration (usually 0.5–1.0mM). These concentrations are much higher than the maximum plasma level reached in humans ($C_{max}$ = 50μM; Kasturi *et al.*, 1998) and so they may

not be physiologically relevant with respect to concentrations attained in target organs(s) of toxicity-susceptible animals.

Despite these limitations, a plausible hypothesis is that CYP4B1 is primarily responsible for catalyzing IPO bioactivation in the lung (and the kidney) of rodents. Support for this view is provided by an *in vivo* study in rats, wherein *p*-xylene, a chemical inhibitor of CYP4B1, protected rats against lung damage induced by IPO (Verschoyle *et al.*, 1993). In mice, IPO is a renal and pulmonary toxin in males but causes only lung damage in females (Boyd, 1976; Boyd *et al.*, 1978). The gender dependency in target organ toxicity in mice mimics the expression pattern of murine CYP4B1, which is regulated by androgens in the kidney (Degawa *et al.*, 1990; Isern and Meseguer, 2003). However, this association must be viewed with caution because CYP2E1 is also expressed in a male-specific fashion in mice (Speerschneider and Dekant, 1995). Therefore, to unambiguously determine the role, in mice, of CYP4B1 in pulmonary and renal damage caused by IPO, we deleted the murine *Cyp4b1* gene and compared the effects of IPO in *Cyp4b1*$^{+/+}$ and *Cyp4b1*$^{-/-}$ mice.

## MATERIALS AND METHODS

***Chemicals.*** NAC, NAL, 1-[(3-cholamidopropyl) dimethylamino]-1-propanesulfate, β-glucuronidase, 4-methylumbelliferone glucuronide, NADPH, UDPGA, $MgCl_2$, EDTA, potassium ferricyanide, potassium ferrocyanide, and X-gal were purchased from Sigma–Aldrich (St Louis, MO). IPO was a gift from the National Cancer Institute (Bethesda, MD). HET0016 (N′-hydroxy-N-(4-n-butyl-2-methylphenyl) formamidine) was provided by Ms Kayte Edson (University of Washington). Goat α-CYP4B1 IgG (raised against rabbit CYP4B1) was a kind gift of Dr R.M. Philpot (Serabjit-Singh *et al.*, 1979). The antibody was used to visualize the presence of CYP4B protein(s) in microsomes by Western blotting at a dilution of 1:5000 and visualized using a donkey anti-goat IRDye 800CW secondary antibody from LI-COR Biosciences (Lincoln, NE).

***Production and characterization of Cyp4b1*$^{-/-}$ *mice.*** Embryonic stem cells (clone G-01, C57Bl/6 genetic background) bearing a targeted disruption of the *Cyp4b1* gene were obtained from the knockout mouse project (KOMP) repository (http://www.komp.org/, University of California, Davis, CA). The cells were expanded on mouse embryonic feeder cells and chimeric mice were generated with the assistance of the UW Transgenic Core Facility (Warren Ladiges, DVM, Director). In brief, embryonic stem cells (15–20) were injected into host albino C57Bl/6 blastocysts and implanted into pseudopregnant female CD-1 mice obtained from Jackson Laboratories (Bar Harbor, ME). The resultant offspring (80 to > 95% coat color chimerism) were backcrossed to albino C57Bl/6 mice to test for germline transmission. Evidence of germline transmission by black coat color was used to select animals for *Cyp4b1* genotyping; heterozygous *Cyp4b1*$^{+/-}$ mice were intercrossed to generate *Cyp4b1*$^{-/-}$ knockouts. The targeting vector designed by CSD/KOMP includes a splice acceptor-beta galactosidase (*lacZ*) reporter just downstream of exon 1 of the *Cyp4b1* gene (Fig. 1). This abolishes CYP4B1 function while placing *lacZ* expression under the control of the mouse *Cyp4b1* gene promoter. To date, more than five generations of knockout mice have been propagated with no overt phenotype and normal viability/fertility.

***Cyp4b1 genotyping.*** Primers were designed to detect the lacZ reporter and the disruption of the *Cyp4b1* gene and purchased from Integrated DNA Technologies (San Diego, CA). Specifically, lacZ primers assessed the presence of the beta-galactosidase reporter gene, and Cyp4b1 primers assessed the presence of wild-type *Cyp4b1*.

DNA was isolated from tail snips and processed using a DNeasy Blood and Tissue Kit (Qiagen, Valencia, CA). Genes were amplified using hot-start PCR (95°C for 2 min, 94°C for 30 s, 57°C for 30 s, 72°C for 2 min) × 35 cycles, 72°C for 5 min. Amplicons were resolved using 1% agarose gel electrophoresis.

***LacZ staining of Cyp4b1*$^{-/-}$ *tissues.*** Animals were sacrificed by carbon dioxide narcosis followed by exsanguination via cardiac puncture. Liver and kidney sections were removed and placed in fixative (4% paraformaldehyde/PBS pH 7.0). Lungs were fixed by severing the trachea and injecting fixative down through the airway into the lungs to fill and expand the lungs in order to improve visualization of the airways and to ensure penetration of the staining solution into the terminal bronchioles. Tissues were stored for 1 h in fixative at 4°C followed by 3 × 30 min rinses with PBS at room temperature. Tissues were then stained for 24 h in staining solution (0.5mM potassium ferricyanide, 0.5mM potassium ferrocyanide, and 1 mg/ml X-gal) at room temperature. Tissues were then rinsed in PBS and fixed overnight in 10% formalin at 4°C.

***Real-time PCR analysis of CYP4B1 expression.*** Comparison of *Cyp4b1* gene expression across tissues in wild-type male and female C57Bl/6 adult mice ($n$ = 3) was determined by real-time (RT) PCR using the ΔΔCt method with 18S as the housekeeping gene. The Taqman primers and probe for each gene were purchased from Applied Biosystems (Foster City, CA). In brief, total RNA was isolated using Tri-reagent (Invitrogen, Carlsbad, CA) and quantified spectrophotometrically. For cDNA synthesis, 1 μg RNA was mixed with Applied Biosystem's Taqman reverse transcription kit utilizing random hexamer primers. The equivalent of 100 ng total RNA was amplified in each RT-PCR reaction with triplicates for each gene. Values are normalized to male lung CYP4B1 expression. Genes were amplified using hot-start PCR (95°C for 10 min followed by 40 cycles of 95°C for 15 s, 60°C for 60 s).

***Western blot analysis of cytochrome P450 expression.*** To confirm that disruption of the *Cyp4b1* gene eliminated expression of CYP4B1 while not affecting expression of other P450 enzymes, we conducted Western blot analysis comparing WT and knockout tissue probed for various P450 enzymes in liver, kidney, and lung microsomes. Tissue microsomes were prepared by differential centrifugation according to previously published protocols (Guengerich, 1994) from frozen tissue pooled from five animals. Microsomal samples were diluted in NuPAGE sample reducing agent and sample buffer from Invitrogen. Microsomal protein (20 μg) was separated on a 4–12% Bis-Tris gel and transferred to a nitrocellulose membrane. Membranes were blocked overnight at 4°C in Odyssey blocking buffer obtained from LI-COR Biosciences followed by probing with 1° antibody (α-CYP2F2, α-CYP1A, α-CYP3A, α-CYP2B, and α-CYP2A) from Santa-Cruz Biotech (Santa Cruz, CA), α-CYP2E and α-CYP2D from Gentest (San Jose, CA), and α-CYP4B1 in blocking buffer and 0.1% Tween at room temperature for 60 min. Membranes were washed three times for 5 min each in PBS followed by incubating with the species-appropriate IRDye 800 CW secondary antibody in blocking buffer and 0.1% Tween for 1 h. Membranes were washed three times for 5 min each in PBS and dried followed by visualization on an Odyssey imaging system.

***IPO toxicity study* in vivo *in Cyp4b1*$^{-/-}$ *mice.*** All protocols involving the use of animals were approved by the Institutional Animal Care and Use Committee at the University of Washington (Seattle, WA) and were performed in accordance with the NIH Guide for the Use and Care of Laboratory Animals. C57Bl/6 mice were obtained from Jackson Laboratories (Bar Harbor, ME). The study design consisted of four mice per group, with age-matched (8–10 weeks of age) male and female *Cyp4b1*$^{-/-}$ or *Cyp4b1*$^{+/+}$ genotypes, and the experiment was performed in duplicate. Animals were kept on a 12-h light/dark cycle and provided water and rodent chow *ad libitum*. Animals were weighed and given 20 mg/kg IPO IP at hour 0 and moved to metabolic cages for urine collection and monitored hourly for signs of distress. The dose of 20 mg/kg was based on studies conducted by Dutcher & Boyd, comparing the ip $LD_{50}$ values across multiple mouse strains (Dutcher and Boyd, 1979). The A/J strain exhibited the lowest $LD_{50}$ of 20 mg/kg, while 25 mg/kg was determined for C57Bl/6; to minimize risk of death while retaining toxicity, 20 mg/kg was selected in conjunction with close monitoring of animal behavior including ambulation and respiration. Mice were sacrificed by carbon dioxide narcosis followed by exsanguination at hour 18. Liver, kidney, and lung were harvested and fixed in formalin (as described for lacZ staining) for histopathological scoring.

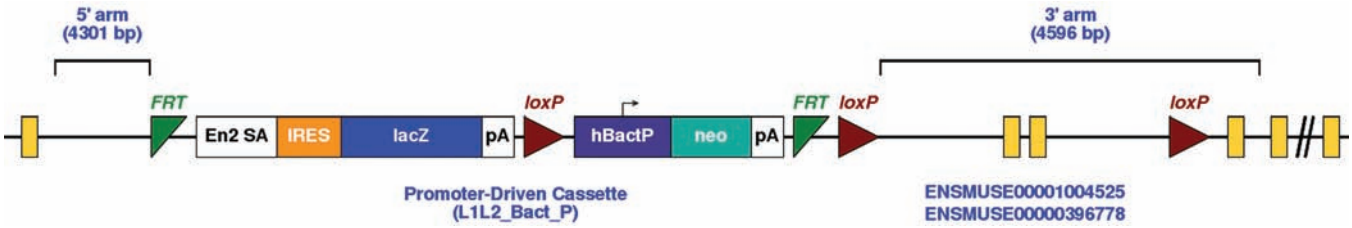


**FIG. 1.** Knockout mouse vector. The target vector was constructed by CSD as part of the NIH KOMP. The targeting vector design by CSD/KOMP includes a splice acceptor-beta galactosidase (*lacZ*) reporter just downstream of exon 1 of the *Cyp4b1* gene. This abolishes CYP4B1 expression while placing *lacZ* expression under the control of the mouse *Cyp4b1* gene promoter (http://www.knockoutmouse.org/martsearch/project/30462).

Heparinized plasma was collected by centrifuging collected blood at 13,000 × g for 5 min. Urine was prepared for analysis by centrifugation for 10 min at 4000 × g and filtered through a sterile 0.2-μM polyethersulfone filter.

**In vitro *bioactivation of IPO by mouse tissues.*** *In vitro* bioactivation of IPO was assessed by incubating microsomal preparations in triplicate with IPO (50μM), potassium phosphate buffer (100mM pH 7.4), NADPH (1mM), EDTA (1mM), $MgCl_2$ (3mM), and NAC and NAL (20mM each). All metabolic incubations were allowed to proceed for 20 min at 37°C in a shaking water bath with a final incubation volume of 200 μl and final protein concentration of 0.2 mg/ml. Reactions were terminated by the addition of an equal volume of ice-cold methanol containing the internal standard, furafylline, and centrifuged

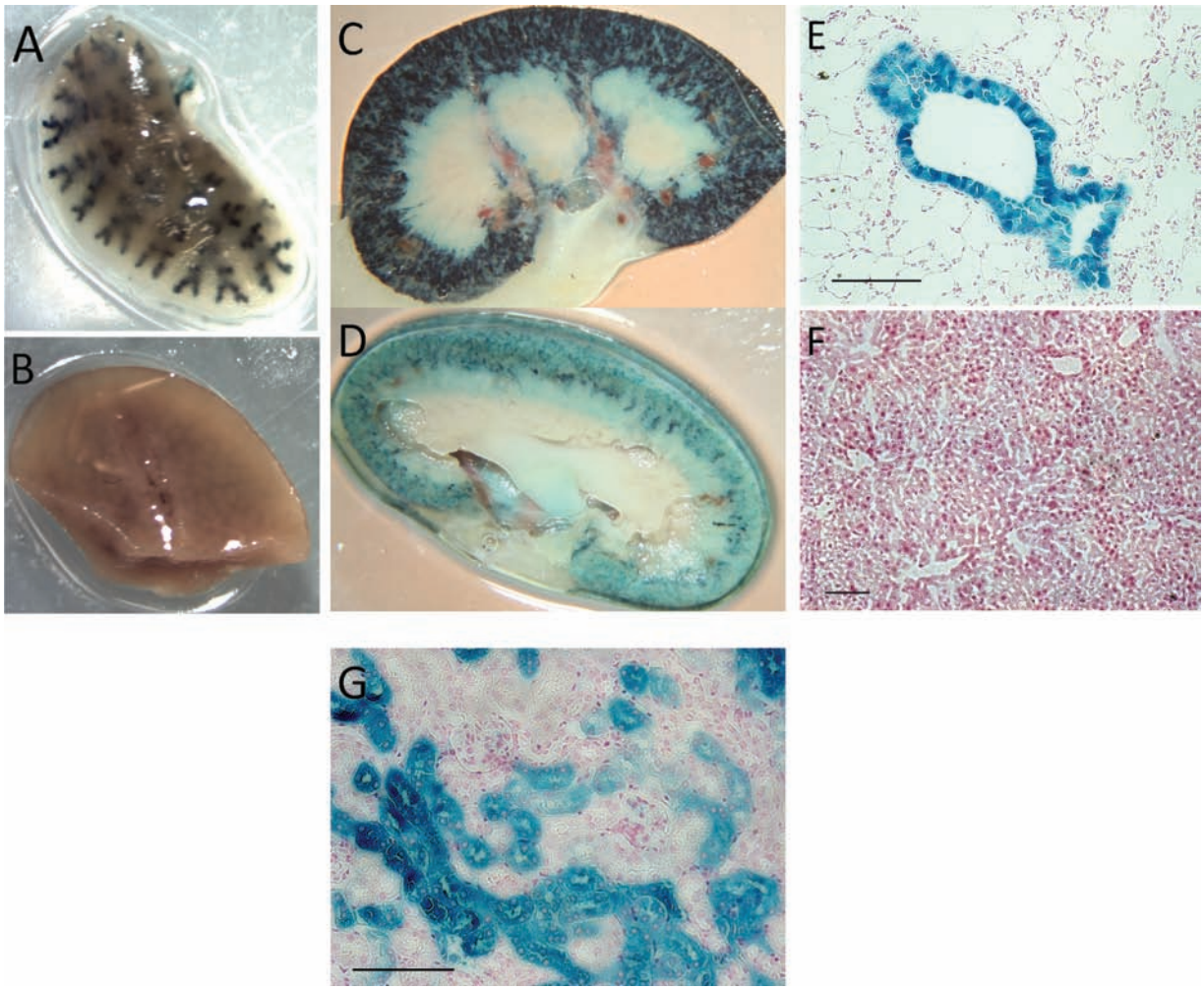


**FIG. 2.** Whole-mount (A–D) and microscopic (E–G) imaging of lung, liver, and kidney from *Cyp4b1*$^{-/-}$ mice stained with the chromogenic substrate X-gal. (A) Whole-mount staining of lung lobe: LacZ activity was readily apparent in Clara cell-rich bronchi and bronchioles. (B) Whole-mount staining of liver lobe: no visible LacZ activity. (C) Whole-mount staining of male (C) and female (D) mouse kidney showing localization of *lacZ/Cyp4b1* expression in the cortex. (E) Microscopic evaluation of mouse lung section shows that expression is restricted to bronchioles and absent from alveoli. (F) Microscopic evaluation of liver section indicates no LacZ activity. (G) Microscopic evaluation of the kidney revealed specific localization to the proximal convoluted tubule. (For E–G, sections were counterstained with Nuclear FastRed; bar = 100μM.)

for 10 min at 4000 rpm to remove protein. Activation rates were assessed by monitoring fragmentation of the NAC/NAL adduct at *m/z* 353 by LC/MS/MS on a Micromass Quattro II tandem quadrupole mass spectrometer operating in positive electrospray mode. The mass spectrometer was coupled to a Shimadzu LC system equipped with a 3-µm particle size Thermo Hypersil gold 100 × 2.1 mm column. Samples were eluted with 10mM formic acid in water (aqueous phase, A) and 10mM formic acid in methanol (organic phase, B) at a flow rate of 300 µl/min. The initial conditions were 70% solvent A and 30% solvent B, which increased to 100% solvent B between 2 and 4 min and remained at 100% solvent B until the end of the run at 5 min. IPO eluted at 4.4 min and was monitored at *m/z* 191 (sodiated IPO) with a cone voltage of 65 V and collision energy of 30 V. The NAC/NAL-IPO adduct eluted at 4.7 min and was monitored by fragmentation at *m/z* 482 > 352, which represents loss of water from the M+H ion (Baer *et al.*, 2005). The internal standard, furafylline, eluted at 4.55 min and was monitored by fragmentation of the parent *m/z* 261.3 > 80.5 at a cone voltage of 35 V and collision energy of 25 V.

## RESULTS

Genotyping of CYP4B1 mice confirmed the presence of the *lacZ* locus and disruption of the native *Cyp4b1* gene (data not shown). To demonstrate targeted expression of the vector, we performed X-gal staining on tissues harvested from *Cyp4b1*$^{-/-}$ animals. Whole-mount visualization of mouse lung (Fig. 2A) indicated that pulmonary expression of β-galactosidase/(CYP4B1) was limited to the airways. Microscopic inspection demonstrated further (Fig. 2E) that expression was limited to Clara cell–rich bronchi and bronchioles, which is characteristic of CYP4B1 (Verschoyle *et al.*, 1993). Staining of kidneys harvested from *Cyp4b1*$^{-/-}$ mice indicated that expression of β-galactosidase followed the same pattern as expression of CYP4B1 in wild-type mice. Expression was restricted to the cortex and was significantly higher in male mice (Fig. 2C) than female mice (Fig. 2D), indicating that renal expression of the reporter is androgen dependent and localized to the same sites of expression as wild-type CYP4B1. Microscopic localization within the cortex was primarily in proximal convoluted tubules, with no evidence for glomeruli staining (Fig. 2G). As expected, no staining was observed in liver (Figs. 2B and 2F).

As expected, RT-PCR and Western blot analysis of CYP4B1 in *Cyp4b1*$^{+/+}$ mouse tissues demonstrated robust expression in female lung and in male lung and kidney (Table 1 and Fig. 3). In contrast, *Cyp4b1*$^{-/-}$ mice exhibited no immunodetectable CYP4B1 in any tissue. It is worth noting that there is a faint band in liver microsomes from both wild-type and knockout mice and this likely represents cross-reactivity with one of the eight members of the *Cyp4a* gene family, which share ~50% protein sequence identity with CYP4B1. In addition, wild-type mice have extremely low levels of hepatic mRNA (Table 1) and there is a complete absence of lacZ reporter activity in

**TABLE 1**
***Cyp4b1* Gene Expression in Various Tissues in Male and Female C57Bl/6 Mice**

| | Relative *Cyp4b1* tissue gene expression | | |
|---|---|---|---|
| Sex | Lung | Kidney | Liver |
| Male | 1.00 (0.63–1.59) | 1.32 (1.21–1.43) | 0.004 (0.002–0.005) |
| Female | 0.67 (0.57–0.80) | 0.16 (0.15–0.17) | 0.008 (0.006–0.009) |

*Note.* RNA was collected from tissues from three 8-week-old mice of each sex. Expression levels (average with range in parentheses defined as $2^{-\Delta\Delta Ct \pm SD}$) are reported relative to male lung *Cyp4b1* expression which is set at 1.0 with 18S rRNA as the housekeeping gene.

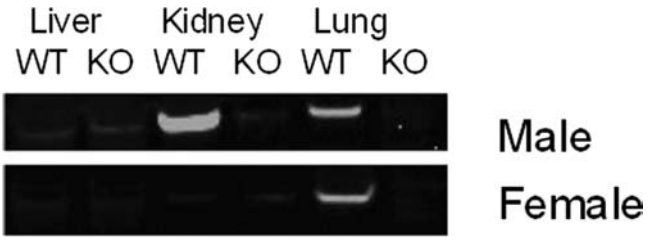


**FIG. 3.** Western blots of mouse liver, kidney, and lung microsomes harvested from *Cyp4b1*$^{+/+}$ and *Cyp4b1*$^{-/-}$ mice (pool of 5) probed with goat α-rabbit CYP4B1 antibody (20 µg microsomal protein added per well). CYP4B1 is highly expressed in the lung of male and female wild-type mice and the kidney of wild-type male mice.

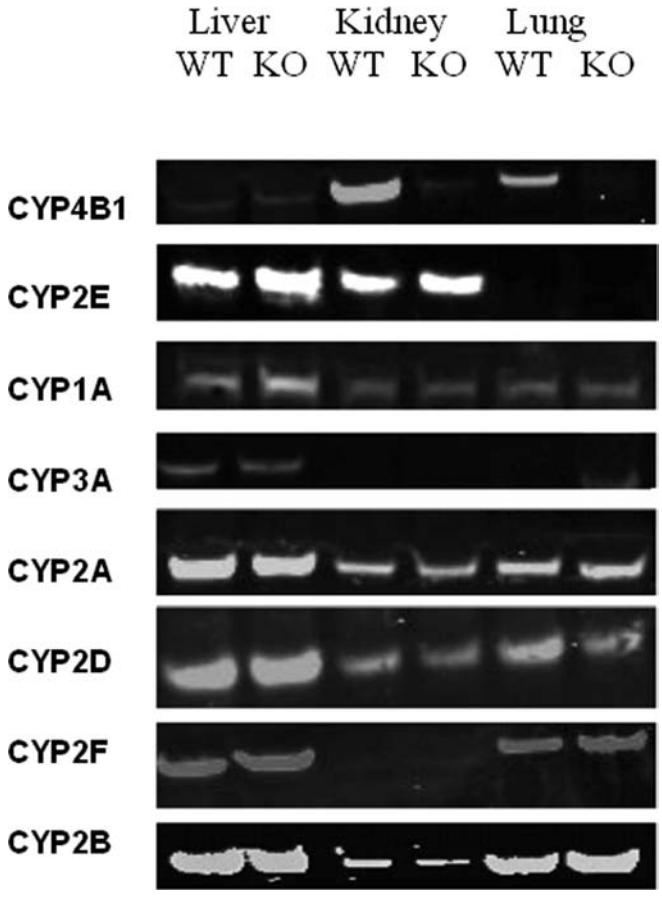


**FIG. 4.** Immunoblots of mouse liver, kidney, and lung microsomes harvested from *Cyp4b1*$^{+/+}$ (WT) and *Cyp4b1*$^{-/-}$ (KO) mice (20 µg microsomal protein added per well) probed with antibodies against selected P450 enzymes as noted and described in "Materials and Methods" section (20 µg microsomal protein added per well). Disruption of *Cyp4b1* did not lead to significant changes in the expression of other P450 enzymes.

**TABLE 2**
***In Vitro* Bioactivation of IPO by Mouse Tissues**

| | IPO bioactivation (pmol/mg/min) | | | | | |
|---|---|---|---|---|---|---|
| | Male liver | Male kidney | Male lung | Female liver | Female kidney | Female lung |
| *Cyp4b1* (+/+) | 18 ± 0.9 | 230 ± 40.2 | 57 ± 5.9 | 21 ± 7.5 | 1.0 ± 0.2 | 73 ± 7.3 |
| *Cyp4b1* (–/–) | 14 ± 1.8 | 1.5 ± 0.34 | 5.8 ± 0.2 | 22 ± 1.4 | 2.4 ± 2.0 | 3.3 ± 1.1 |

*Note.* *Cyp4b1*$^{-/-}$ mice exhibited > 90% decrease in microsomal IPO activation by male and female lung and male kidney, but no change in activation rates in liver where CYP4B1 is not expressed.

knockout livers (Fig. 2F). This confirms that disruption of the *Cyp4b1* gene by the targeting vector resulted in an absence of expression of CYP4B1 protein.

Western blot analysis of P450 expression in mouse tissue microsomes from male *Cyp4b1*$^{+/+}$ and *Cyp4b1*$^{-/-}$ animals demonstrated further that there was no significant compensatory upregulation in the expression of CYP1A, CYP2A, CYP2B, CYP2D, CYP2E, CYP3A, or CYP2F enzymes in lung, liver, or kidney as a result of disruption of the *Cyp4b1* locus (Fig. 4).

IPO-adduct formation rates in microsomes from tissue harvested from *Cyp4b1*$^{-/-}$ and *Cyp4b1*$^{+/+}$ mice suggest strongly that CYP4B1 plays a significant role in the bioactivation of IPO in murine lung and kidney. NAC/NAL adduct formation rates were highest in male renal microsomes followed by male and female pulmonary microsomes; data that correlate well with the CYP4B1 content of microsomes are given in Table 2.

Finally, results from the *in vivo* study demonstrate that loss of CYP4B1 function is protective in mice exposed to

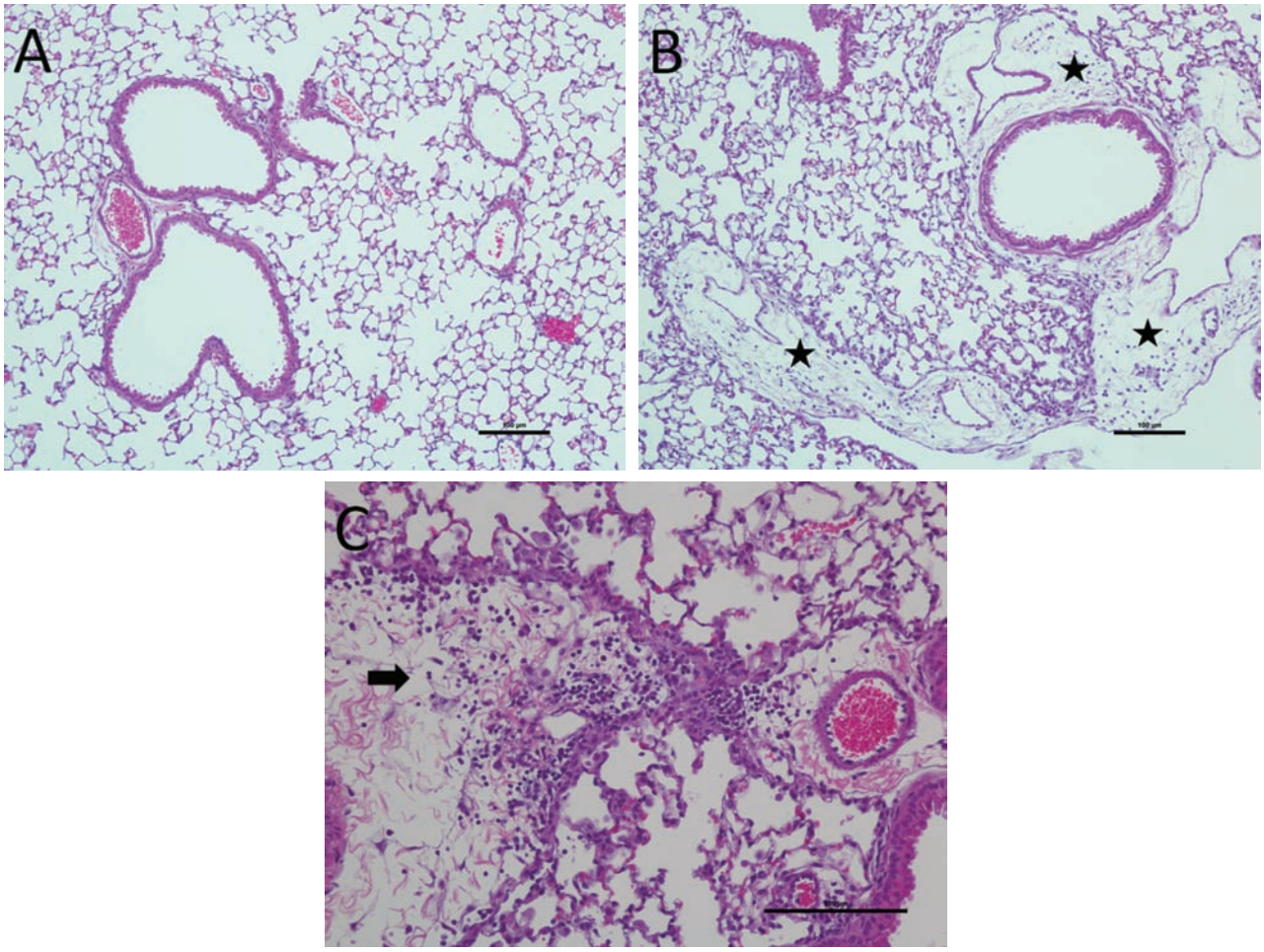


**FIG. 5.** Lung histopathology of mice treated with 20 mg/kg IPO. (A) *Cyp4b1* null mice exhibit no overt signs of toxicity. (B and C) Wild-type *Cyp4b1* mice. In (B), stars indicate significantly widened perivascular spaces. These spaces contain engorged lymphatics and extravascular fluid (washed out in processing) as well as scattered mononuclear inflammatory cells and some fine fibrin strands. In (C), the arrow indicates significantly widened perivascular space containing a focal cluster of mononuclear inflammatory cells. Surrounding alveolar walls are also slightly thickened by inflammatory cell and fluid accumulations (hematoxylin/eosin stain, bar = 100μM).

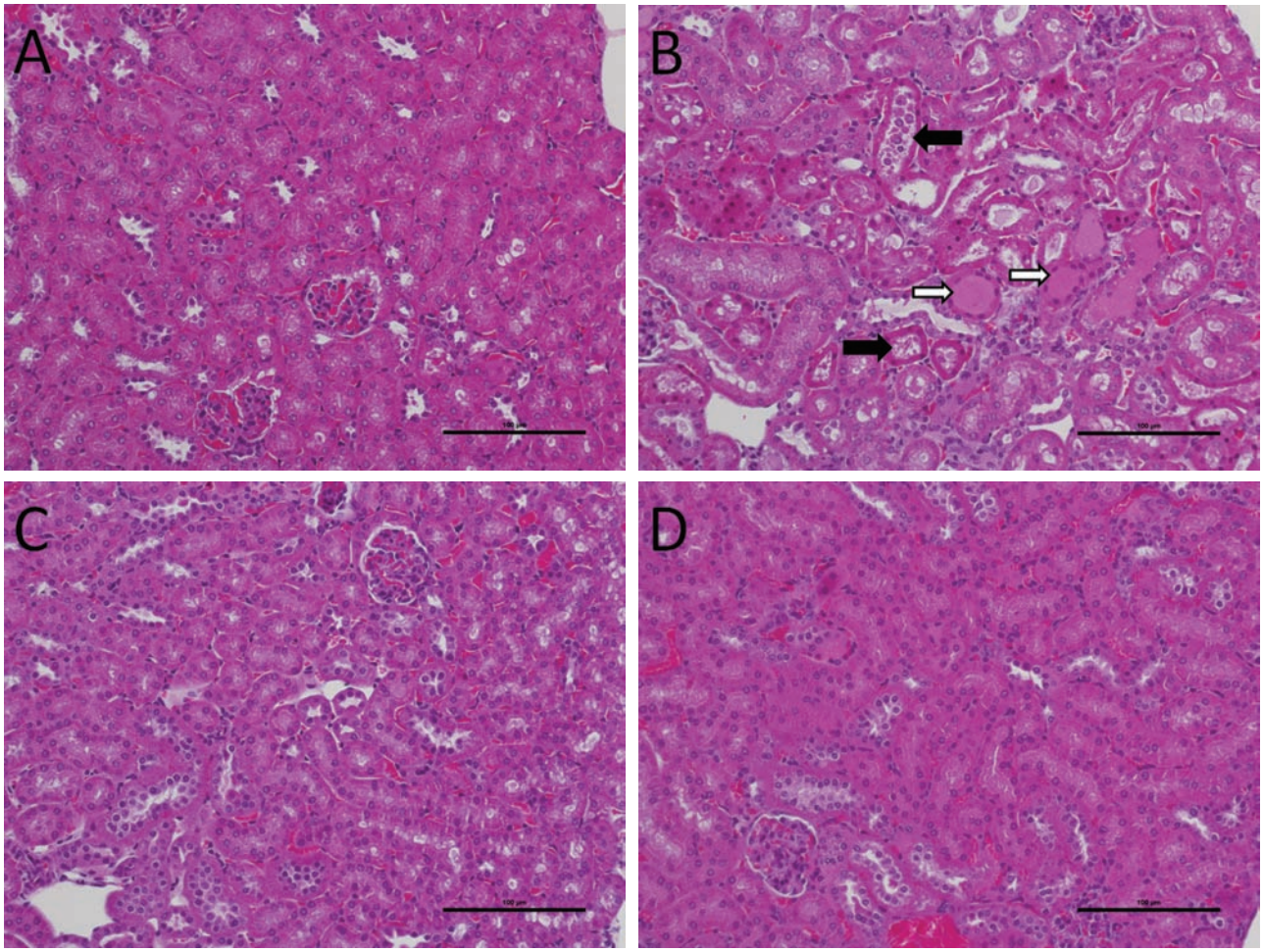


**FIG. 6.** Histology of IPO-treated mouse kidney. (A) *Cyp4b1*$^{-/-}$ male mouse kidney. *Cyp4b1*$^{-/-}$ mice exhibit no overt signs of toxicity. (B) The kidneys of *Cyp4b1*$^{+/+}$ male mice showed signs of proteinurea (white arrows) and widespread necrotic and sloughed epithelium (black arrows). Kidney from female *Cyp4b1*$^{-/-}$ (C) and *Cyp4b1*$^{+/+}$ (D) mice. Females of both genotypes showed no overt signs of toxicity (hematoxylin/eosin stain, bar = 100μM).

IPO (Fig. 5A). When treated with 20 mg/kg IPO, *Cyp4b1*$^{+/+}$ mice developed pulmonary lesions characterized by significantly widened perivascular/peribronchiolar spaces containing engorged lymphatics and extravascular fluid, as well as fibrin strands (Fig. 5B). *Cyp4b1*$^{+/+}$ mice also displayed scattered, focal thickening of alveolar walls and accumulation of mononuclear cells into perivascular space (Fig. 5C). Similar lesions were not evident in *Cyp4b1*$^{-/-}$ mice, indicating that CYP4B1 is required for bioactivation of IPO *in vivo*.

Consistent with androgen-mediated kidney expression of CYP4B1, we observed moderate renal toxicity in two of the four IPO-treated *Cyp4b1*$^{+/+}$ male mice, which was not evident in female mice of either genotype (Figs. 6C and D) or male *Cyp4b1*$^{-/-}$ mice (Fig. 6A). The cortices of affected kidneys were characterized histologically by several changes which principally affected renal tubular epithelium (Fig. 6B). These changes included frequent condensation of renal tubular epithelium sometimes closely adjacent to swollen and vacuolated tubular epithelium. In addition, there was widely scattered necrosis and sloughing of tubule lining cells. Occasional accumulation of dark pink proteinaceous fluid within tubule lumens is consistent with some degree of glomerular injury although histological changes to glomerular tufts were not noticeable.

## DISCUSSION

We have generated a *Cyp4b1*$^{-/-}$ mouse utilizing a targeting vector designed by CSD/KOMP that includes a splice acceptor-β-galactosidase (*lacZ*) reporter just downstream of exon 1 of the *Cyp4b1* gene (Fig. 1). This abolishes CYP4B1 function while placing *lacZ* expression under the control of the mouse *Cyp4b1* gene promoter. We have confirmed disruption of the *Cyp4b1* gene, as well as site-specific expression of *lacZ* at the known sites of CYP4B1 expression, including pulmonary Clara cells and the cortex of male kidneys. Furthermore, there

is no evidence of an altered phenotype in *Cyp4b1*$^{-/-}$ mice relative to wild-type mice.

Predictably, disruption of *Cyp4b1* eliminates protein expression in microsomes of *Cyp4b1*$^{-/-}$ mice. In *Cyp4b1*$^{+/+}$ mice, CYP4B1 is highly expressed in the kidney and lung of males and the lung of females, as evidenced by Western blotting and RT-PCR (Fig. 3 and Table 1). We saw no evidence of CYP4B1 expression in the liver of *Cyp4b1*$^{+/+}$ or *Cyp4b1*$^{-/-}$ mice of either sex. In *Cyp4b1*$^{-/-}$ mice, there was no detectable CYP4B1 protein in any of the tissues we examined. We conclude that we have successfully produced viable *Cyp4b1* null mice with no overt detrimental effects resulting from disruption of the gene.

It is possible that elimination of a P450 enzyme could lead to upregulation of other P450 enzymes to compensate for the disruption of the endogenous functions of the target gene. For example, knockout of CYP3A enzymes in the mouse resulted in a surprising conservation of hepatic midazolam hydroxylation, which was attributed to upregulation of murine CYP2C enzymes (van Waterschoot *et al.*, 2008). Changes in the global P450 expression levels in *Cyp4b1*$^{-/-}$ mice could conceivably mask the loss of target gene activity making utilization of the knockout animal in toxicity studies ineffective should alternative bioactivation pathways exist. To evaluate this possibility, we conducted Western blot analysis of IPO target tissues (kidney and lung) and the liver to determine relative levels of expression of the major P450 families in *Cyp4b1*$^{-/-}$ and *Cyp4b1*$^{+/+}$ mice. Our data indicate that expression of P450 enzymes from the 1A, 2A, 2B, 2D, 2E, and 3A families, as well as expression of CYP2F2, is unaffected by disruption of the *Cyp4b1* locus. Therefore, we can conclude that differences in activation or metabolism of xenobiotics between *Cyp4b1*$^{-/-}$ and *Cyp4b1*$^{+/+}$ mice, as well as differences in toxicity in response to protoxins, are due to the loss of functional CYP4B1 in the *Cyp4b1*$^{-/-}$ mice and do not result from altered expression of other P450 enzymes.

*In vitro* IPO bioactivation rates in murine liver, lung, and kidney generally paralleled protein expression of CYP4B1, in that the highest rates were observed in male and female lung microsomes and male kidney microsomes. IPO bioactivation catalyzed by pulmonary microsomes from *Cyp4b1*$^{-/-}$ mice was decreased by > 90% and almost completely eradicated in renal microsomes from male mice. This highlights the dominance of CYP4B1 in IPO bioactivation in these target tissues *in vitro*. These microsomal results correlate well with the data obtained from the *in vivo* toxicity study in IPO-treated mice. Based on the histopathological evidence, male *Cyp4b1*$^{+/+}$ mice experienced both pulmonary and renal toxicity, whereas female *Cyp4b1*$^{+/+}$ mice experienced only pulmonary toxicity. These sites of toxicity mirror the organs possessing the highest levels of CYP4B1 expression. The observation of nephrotoxicity in male *Cyp4b1*$^{+/+}$ mice is likely specific to rodents, as other species (e.g., rabbits and cows) exhibit only pneumotoxicity, despite robust IPO bioactivation by rabbit liver microsomes (Parkinson *et al.*, 2012). Importantly, *no toxicity* was observed in any *Cyp4b1*$^{-/-}$ mice, indicating that CYP4B1 expression and associated catalytic activity is the primary determinant of IPO-related toxicity in mice.

In conclusion, we have generated the first *Cyp4b1*$^{-/-}$ mouse model and determined that the pulmonary (and renal) toxicity of IPO in mice is a consequence of bioactivation by murine CYP4B1. P450 knockout mice are being used increasingly to probe the enzymatic mechanisms of action of other respiratory tract toxins, including 2,6-dichlorobenzonitrile (Xie *et al.*, 2010), naphthalene (Li *et al.*, 2011), and 3-methylindole (Zhou *et al.*, 2012). It is known that CYP4B1 prefers to metabolize relatively small, aromatic compounds (Baer and Rettie, 2006) and so it will be of interest to evaluate the role of CYP4B1 in the bioactivation of these, and other, protoxins that fit the known substrate selectivity of the enzyme. Finally, given the exquisite tissue specificity of IPO toxicity, and the absolute requirement of CYP4B1 in the bioactivation of this protoxin, the *Cyp4b1*$^{-/-}$ mouse should serve as an excellent model for investigating biomarkers of tissue-specific injury.

## FUNDING

National Institutes of Health (GM49054 to A.E.R., ES007033 to E.J.K.); Brady Fund for Natural Products Research; Drug Metabolism Transport and Pharmacogenetics Research Fund in the School of Pharmacy, University of Washington.

## ACKNOWLEDGMENTS

The authors thank Efriem Bezabih, Mikias Woldetensae, and Kelly Hudkins for technical assistance.

## REFERENCES

Baer, B. R., and Rettie, A. E. (2006). CYP4B1: An enigmatic P450 at the interface between xenobiotic and endobiotic metabolism. *Drug Metab. Rev.* **38,** 451–476.

Baer, B. R., Rettie, A. E., and Henne, K. R. (2005). Bioactivation of 4-ipomeanol by CYP4B1: Adduct characterization and evidence for an enedial intermediate. *Chem. Res. Toxicol.* **18,** 855–864.

Boyd, M. R. (1976). Role of metabolic activation in the pathogenesis of chemically induced pulmonary disease: Mechanism of action of the lung-toxic furan, 4-ipomeanol. *Environ. Health Perspect.* **16,** 127–138.

Boyd, M. R., and Burka, L. T. (1978). In vivo studies on the relationship between target organ alkylation and the pulmonary toxicity of a chemically reactive metabolite of 4-ipomeanol. *J. Pharmacol. Exp. Ther.* **207,** 687–697.

Boyd, M. R., Burka, L. T., Wilson, B. J., and Sasame, H. A. (1978). In vitro studies on the metabolic activation of the pulmonary toxin, 4-ipomeanol, by rat lung and liver microsomes. *J. Pharmacol. Exp. Ther.* **207,** 677–686.

Czerwinski, M., McLemore, T. L., Philpot, R. M., Nhamburo, P. T., Korzekwa, K., Gelboin, H. V., and Gonzalez, F. J. (1991). Metabolic activation of 4-ipomeanol by complementary DNA-expressed human cytochromes P-450: Evidence for species-specific metabolism. *Cancer Res.* **51,** 4636–4638.

Degawa, M., Miura, S., and Hashimoto, Y. (1990). Androgen-dependent renal microsomal cytochrome P-450 responsible for N-hydroxylation and mutagenic activation of 3-methoxy-4-aminoazobenzene in the BALB/c mouse. *Cancer Res*. **50,** 2729–2733.

Devereux, T. R., Jones, K. G., Bend, J. R., Fouts, J. R., Statham, C. N., and Boyd, M. R. (1982). In vitro metabolic activation of the pulmonary toxin, 4-ipomeanol, in nonciliated bronchiolar epithelial (Clara) and alveolar type II cells isolated from rabbit lung. *J. Pharmacol. Exp. Ther*. **220,** 223–227.

Doster, A. R., Mitchell, F. E., Farrell, R. L., and Wilson, B. J. (1978). Effects of 4-ipomeanol, a product from mold-damaged sweet potatoes, on the bovine lung. *Vet. Pathol*. **15,** 367–375.

Dutcher, J. S., and Boyd, M. R. (1979). Species and strain differences in target organ alkylation and toxicity by 4-ipomeanol. Predictive value of covalent binding in studies of target organ toxicities by reactive metabolites. *Biochem. Pharmacol*. **28,** 3367–3372.

Garst, J. E., Wilson, W. C., Kristensen, N. C., Harrison, P. C., Corbin, J. E., Simon, J., Philpot, R. M., and Szabo, R. R. (1985). Species susceptibility to the pulmonary toxicity of 3-furyl isoamyl ketone (perilla ketone): In vivo support for involvement of the lung monooxygenase system. *J. Anim. Sci*. **60,** 248–257.

Guengerich, F. P. (1994). Analysis and characterization of enzymes. In *Principles and Methods of Toxicology* (A. W. Hayes, Ed.), pp. 1259–1313. Raven Press, New York, NY.

Isern, J., and Meseguer, A. (2003). Hormonal regulation and characterisation of the mouse Cyp4b1 gene 5'-flanking region. *Biochem. Biophys. Res. Commun*. **307,** 139–147.

Kasturi, V. K., Dearing, M. P., Piscitelli, S. C., Russell, E. K., Sladek, G. G., O'Neil, K., Turner, G. A., Morton, T. L., Christian, M. C., Johnson, B. E., *et al.* (1998). Phase I study of a five-day dose schedule of 4-Ipomeanol in patients with non-small cell lung cancer. *Clin. Cancer Res*. **4,** 2095–2102.

Li, L., Wei, Y., Van Winkle, L., Zhang, Q. Y., Zhou, X., Hu, J., Xie, F., Kluetzman, K., and Ding, X. (2011). Generation and characterization of a Cyp2f2-null mouse and studies on the role of CYP2F2 in naphthalene-induced toxicity in the lung and nasal olfactory mucosa. *J. Pharmacol. Exp. Ther*. **339,** 62–71.

Parkinson, O. T., Kelly, E. J., Bezabih, E., Whittington, D., and Rettie, A. E. (2012). Bioactivation of 4-Ipomeanol by a CYP4B enzyme in bovine lung and inhibition by HET0016. *J. Vet. Pharmacol. Ther*. **35,** 402–405.

Serabjit-Singh, C. J., Wolf, C. R., and Philpot, R. M. (1979). The rabbit pulmonary monooxygenase system. Immunochemical and biochemical characterization of enzyme components. *J. Biol. Chem*. **254,** 9901–9907.

Speerschneider, P., and Dekant, W. (1995). Renal tumorigenicity of 1,1-dichloroethene in mice: The role of male-specific expression of cytochrome P450 2E1 in the renal bioactivation of 1,1-dichloroethene. *Toxicol. Appl. Pharmacol*. **130,** 48–56.

van Waterschoot, R. A., van Herwaarden, A. E., Lagas, J. S., Sparidans, R. W., Wagenaar, E., van der Kruijssen, C. M., Goldstein, J. A., Zeldin, D. C., Beijnen, J. H., and Schinkel, A. H. (2008). Midazolam metabolism in cytochrome P450 3A knockout mice can be attributed to up-regulated CYP2C enzymes. *Mol. Pharmacol*. **73,** 1029–1036.

Verschoyle, R. D., Philpot, R. M., Wolf, C. R., and Dinsdale, D. (1993). CYP4B1 activates 4-ipomeanol in rat lung. *Toxicol. Appl. Pharmacol*. **123,** 193–198.

Wolf, C. R., Statham, C. N., McMenamin, M. G., Bend, J. R., Boyd, M. R., and Philpot, R. M. (1982). The relationship between the catalytic activities of rabbit pulmonary cytochrome P-450 isozymes and the lung-specific toxicity of the furan derivative, 4-ipomeanol. *Mol. Pharmacol*. **22,** 738–744.

Xie, F., Zhou, X., Behr, M., Fang, C., Horii, Y., Gu, J., Kannan, K., and Ding, X. (2010). Mechanisms of olfactory toxicity of the herbicide 2,6-dichlorobenzonitrile: Essential roles of CYP2A5 and target-tissue metabolic activation. *Toxicol. Appl. Pharmacol*. **249,** 101–106.

Zhou, X., D'Agostino, J., Li, L., Moore, C. D., Yost, G. S., and Ding, X. (2012). Respective roles of CYP2A5 and CYP2F2 in the bioactivation of 3-methylindole in mouse olfactory mucosa and lung: Studies using Cyp2a5-null and Cyp2f2-null mouse models. *Drug Metab. Dispos*. **40,** 642–647.